JOURNAL OF SPACECRAFT AND ROCKETS
Vol. 42, No. 2, March–April 2005

Engineering Notes

ENGINEERING NOTES are short manuscripts describing new developments or important results of a preliminary nature. These Notes cannot exceed six manuscript pages and three figures; a page of text may be substituted for a figure and vice versa. After informal review by the editors, they may be published within a few months of the date of receipt. Style requirements are the same as for regular contributions (see inside back cover).

Dynamics of Rotating Linear Array Tethered Satellite System

K. D. Kumar* and T. Yasaka†
Kyushu University, Fukuoka 812-8581, Japan

Nomenclature

a_{ij}, b_{ij}, c_{ij}	=	x_i, y_i, z_i coordinates of the offset points of tether j in satellite i, m
$\hat{a}_{ij}, \hat{b}_{ij}, \hat{c}_{ij}, \hat{b}_j$	=	a_{ij}/L_{ref}, b_{ij}/L_{ref}, c_{ij}/L_{ref}, and $\lvert\hat{b}_{jj}\rvert$ or $\lvert\hat{b}_{(j+1)j}\rvert$ when $\lvert\hat{b}_{jj}\rvert = \lvert\hat{b}_{(j+1)j}\rvert$, $j = 1, 2$
C	=	$EA/(m_2 L_{\text{ref}}\Omega^2)$, where EA is tether modulus of rigidity, N
e	=	orbital eccentricity
f_i, g_i	=	satellite mass and moment of inertia ratios, m_1/m_{i+1}, $I_{x1}/I_{x(i+1)}$
K_{i1}, K_{i2}	=	$(I_{xi} - I_{yi})/I_{zi}$, $(I_{xi} - I_{zi})/I_{yi}$; $K_1 = K_{i1}$, $K_2 = K_{i2}$; when $K_{j1} = K_{(j+1)1}$, $K_{j2} = K_{(j+1)2}$, $j = 1, 2$
L_j	=	distance between satellite mass centers S_j and S_{j+1}, m
L_{j0}, L_{ref}	=	unstretched jth tether length, m, and reference length, $(I_{x1}/m_2)^{1/2}$, m
L^s_{j0}, L^f_{j0}	=	initial and final unstretched jth tether length during deployment/retrieval, m
L_{t0}, L^e_{t0}	=	L_{j0}, L^e_{j0}, $j = 1, 2$, when $L_{k0} = L_{(k+1)0}$, $L^e_{k0} = L^e_{(k+1)0}$, $k = 1, 2$, m
l_j, l_{j0}	=	$L_j/L_{\text{ref}}, L_{j0}/L_{\text{ref}}$
m_i, I_{ki}	=	mass, kg, and principal moment of inertia of satellite i about k_i axis, $k = x, y, z$, kgm^2
$\hat{Q}_q$	=	$Q_q/(m_2 L_{\text{ref}}\Omega^2)$, where Q_q is the generalized force corresponding to generalized coordinate q
r_{ij}	=	radial jth tether offset $S_i E_i$ at satellite i from its mass center S_i (Fig. 1), m
$\hat{r}_{ij}, \hat{r}_b$	=	r_{ij}/L_{ref} and $\hat{r}_{jj}$ or $\hat{r}_{(j+1)j}$ when $\hat{r}_{jj} = \hat{r}_{(j+1)j}$, $j = 1, 2$
θ, θ_{j0}	=	true anomaly and θ when jth tether deployment/retrieval starts, deg
τ_j	=	orbits for the completion of deployment/retrieval of jth tether; $\tau_j = \tau$ if $\tau_k = \tau_{k+1}$, $k = 1, 2$
χ_i	=	relative pitch attitude angle of the satellite i with respect to in-plane swing angle β_j; $\alpha_i - \beta_j$, $i = 1, 2, 3$; $j = 1$ if $i = 1, 2$; $j = 2$ if $i = 3$, deg
Ω	=	mean orbital rate

Subscripts

max	=	absolute maximum amplitude
0	=	at $\theta = 0$

Superscripts

e	=	at equilibrium
$', ''$	=	$\mathrm{d}(\cdot)/\mathrm{d}\theta$ and $\mathrm{d}^2(\cdot)/\mathrm{d}\theta^2$, respectively

Introduction

THE application of tethers[1–6] represents one of the important concepts necessary to achieve satellite formation flying with minimum stationkeeping requirements. DeCou,[1] Tragesser,[2] and Williams and Moore[3] have studied the dynamics of a rotating triangular formation of three-body tethered satellite systems (TSS). Quadrelli[4] described a general simulation model to predict the dynamics and control performance of formations of a two-body TSS in a heliocentric or low Earth orbit. Bombardelli et al.[5] analyzed the pointing dynamics of a three-body-on-line tethered interferometer orbiting an Earth-trailing, heliocentric orbit. In the present investigation, we consider finite end masses instead of point end masses, along with the tether deployment/retrieval, for a rotating linear array TSS in an Earth-centered elliptic orbit. The major contributions are the derivation of tether deployment and retrieval criteria to guarantee the steady-spin motion of the TSS, the analysis of the effects of tether length/offset and tether flexibility on the TSS response, and the synthesis of tether offset and tension control laws to achieve desired tether deployment/retrieval.

Proposed System Model and Equations of Motion

The system model comprises two or three satellites connected by flexible tethers at a point on each satellite with offsets (Fig. 1). The tethers, considered to be made of light material, are assumed to have negligible mass. Their damping effects and transverse vibrations are ignored. Because of the relatively short tether length, the tether dynamics is assumed to have no effect on the orbital dynamics. The nodal line represents the reference line in orbit for the measurement of the true anomaly. The coordinate frame $X_0Y_0Z_0$ passing through the system center of mass S is the orbital reference frame. Here, the X_0 axis is normal to the orbital plane, the Y_0 axis points along the local vertical, and the Z_0 axis represents the third axis of this right-handed frame. The orientation of the satellite i, $i = 1$, 2, 3, is specified by a set of three successive rotations: α_i (pitch) about the X_{i0} axis, ϕ_i (roll) about the Z_{i1} axis, and, finally, γ_i (yaw) about the Y_{i2} axis. The corresponding principal body-fixed coordinate frame is denoted by $S_i - X_iY_iZ_i$. Similarly, for the variable length $\boldsymbol{L}_i$ joining the two satellite mass centers S_i and S_{i+1}, the angle β_i denotes rotation about the axis normal to the orbital plane and is referred to as the in-plane swing angle, whereas the angle η_i represents its out-of-plane swing angle. The resulting coordinate frame associated with $\boldsymbol{L}_i$ is $S_{Li} - X_{Li}Y_{Li}Z_{Li}$. The governing Lagrangian equations of motion[6] after considerable algebraic manipulation and nondimensionalization are carried out are written corresponding to

Received 1 October 2003; revision received 4 November 2004; accepted for publication 12 November 2004.

*Japan Society for the Promotion of Science Fellow, Department of Aeronautics and Astronautics; krishnadevkumar@yahoo.com. Member AIAA.

†Professor, Department of Aeronautics and Astronautics; yasaka@aero.kyushu-u.ac.jp. Member AIAA.

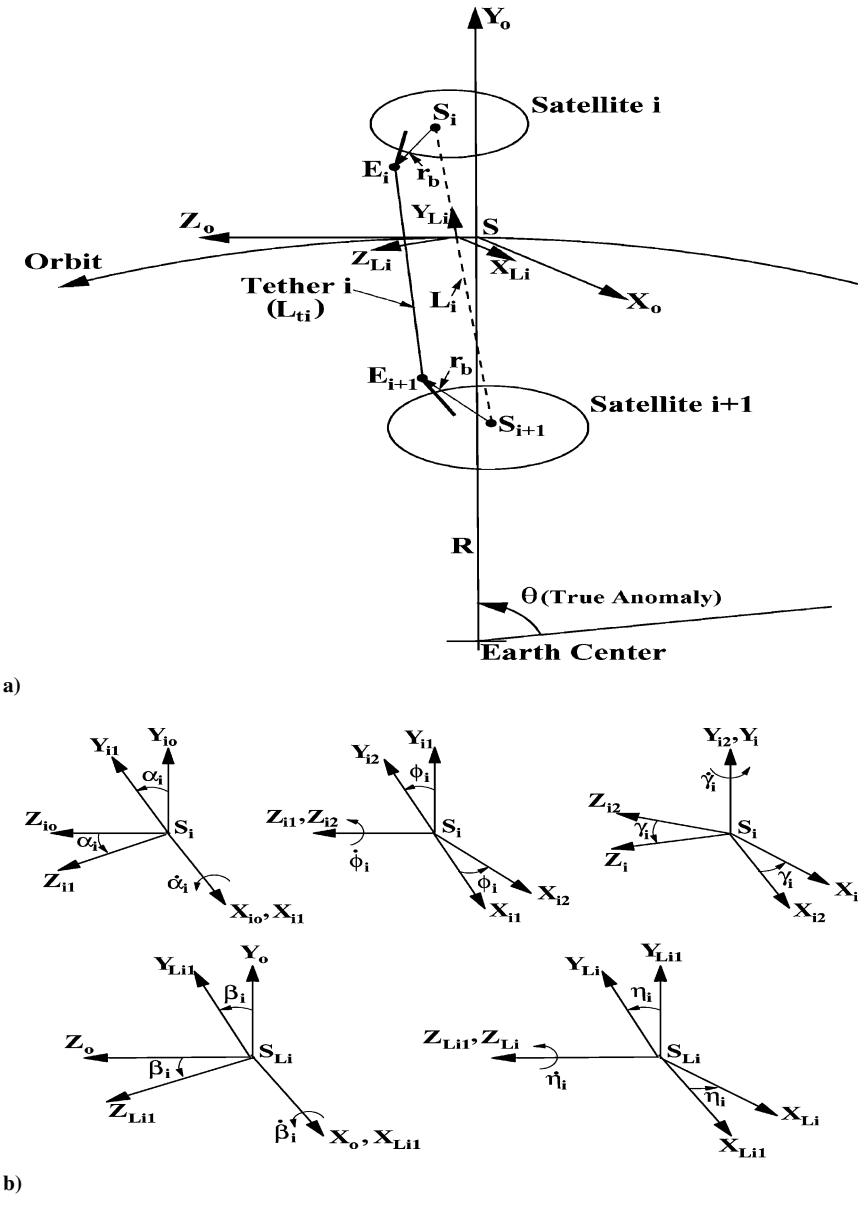

Fig. 1 Geometry of the system model: a) system configuration and b) orientation of the satellite *i* and tether *i* with respect to orbital reference frame.

generalized coordinates $q = (\alpha_i, \phi_i, \gamma_i, L_i, \beta_i, \eta_i, i = 1, 2)^T$ in matrix notations as

$$\boldsymbol{M}(q, \theta, e, K_1, K_2)q'' + \boldsymbol{F}(q, q', \theta, e, K_1, K_2) = \hat{Q}_q \qquad (1)$$

where $\boldsymbol{M}(q, \theta, e, K_1, K_2)$ is the mass matrix and $\boldsymbol{F}(q, q', \theta, e, K_1, K_2)$ is the vector containing all of the nonlinear terms, including the Coriolis and centrifugal contributions.[6] The details of the governing equations of motion are omitted for brevity.

Tether Deployment/Retrieval

We consider the tether deployment/retrieval scheme as follows:

$$l_{j0} = l^s_{j0} + \left(l^f_{j0} - l^s_{j0}\right)\sin[(\theta - \theta_{j0})/4\tau_j]$$

$$\text{if} \quad 0 \le (\theta - \theta_{j0}) < 2\pi\tau_j, \qquad j = 1, 2, 3$$

$$l'_{j0} = \left[\left(l^f_{j0} - l^s_{j0}\right)\Big/4\tau_j\right]\cos[(\theta - \theta_{j0})/4\tau_j]$$

$$\text{if} \quad 0 \le (\theta - \theta_{j0}) < 2\pi\tau_j, \qquad j = 1, 2, 3$$

$$l_{j0} = l^f_{j0} \quad \text{if} \quad 2\pi\tau_j \le (\theta - \theta_{j0}), \qquad j = 1, 2, 3$$

$$l'_{j0} = 0 \quad \text{if} \quad 2\pi\tau_j \le (\theta - \theta_{j0}), \qquad j = 1, 2, 3 \qquad (2)$$

By application of the preceding deployment/retrieval scheme (2), the final commanded tether length deployment/retrieval rate reaches zero, and, thus, the problems of sudden excitation of system response caused at the end of deployment/retrieval can be avoided. To derive the criteria for tether deployment and retrieval to guarantee the steady-spin motion of the TSS, we first analyze the equilibrium conditions, and, thereupon, the TSS spin rate is studied.

TSS Equilibrium Conditions

We assume that the TSS is in an arbitrary instantaneous equilibrium configuration and rotating in an orbital plane given by, for example, $e = 0$, $\alpha_i = \beta_e$, $\phi_i = \gamma_i = 0$, $i = 1, 2, 3$; $\beta_j = \beta_e$, $\beta'_j = \beta'_{je} = \beta'_e$, $\eta_j = \eta'_j = \eta'_{je} = 0$; $j = 1, 2$. On substitution of the instantaneous equilibrium configurations into Eqs. (1), as well as algebraic manipulations and simplification, we obtain the tether strain

ε_{je} and equilibrium distance l_{je} as, for a three-body TSS,

$$\varepsilon_j^e = p_4\left\{\left(d_{j0}^e + \frac{p_3}{p_j}d_{k0}^e\right)\frac{C}{p_k} - p_4 l_{k0}^e\left[d_{j0}^e + \frac{p_3}{p_j}d_{k0}^e + \frac{p_3}{p_j}\left(d_{k0}^e + \frac{p_3}{p_k}d_{j0}^e\right)\right]\right\}\Bigg/\left[\left(\frac{C}{p_j} - p_4 l_{j0}^e\right)\left(\frac{C}{p_k} - p_4 l_{k0}^e\right) - \frac{p_3^2}{p_j p_k}d_{j0}^e d_{k0}^e p_4^2\right], \qquad j = 1, 2$$

$$l_j^e = l_{j0}^e\left(1 + \varepsilon_j^e\right) - \hat{b}_{jj} + \hat{b}_{(j+1)j}, \qquad j = 1, 2 \tag{3}$$

where

$$k = 2 \quad \text{if} \quad j = 1, k = 1 \quad \text{if} \quad j = 2, \quad d_{j0}^e = l_{j0}^e - \hat{b}_{jj} + \hat{b}_{(j+1)j}$$

$$p_1 = \frac{f_1(1 + f_1/f_2)}{1 + f_1 + f_1/f_2}, \qquad p_2 = \frac{(f_1/f_2)(1 + f_1)}{1 + f_1 + f_1/f_2}$$

$$p_3 = \frac{f_1(f_1/f_2)(3 + f_1 + f_1/f_2)}{(1 + f_1 + f_1/f_2)^2}, \qquad p_4 = (1 + \beta_e')^2 - 1 + 3\cos^2\beta_e$$

For a two-body TSS,

$$\varepsilon_1^e = \frac{p_4\left[l_{10}^e - \hat{b}_{11} + \hat{b}_{21}\right]}{C(1 + 1/f_1) - p_4 l_{10}^e}, \qquad l_1^e = \frac{C(1 + 1/f_1)\left[l_{10}^e - \hat{b}_{11} + \hat{b}_{21}\right]}{C(1 + 1/f_1) - p_4 l_{10}^e} \tag{4}$$

For the stable motion of the system, all tethers must remain taut, and, thus, we have the following conditions using Eqs. (3) and (4) for the three-body TSS:

$$C > p_k l_{k0}^e p_5\left[1 + \left(\frac{p_3}{p_j}\right)\frac{d_{k0}^e + (p_3/p_k)d_{j0}^e}{d_{j0}^e + (p_3/p_j)d_{k0}^e}\right]$$

$$j = 1, 2, \quad \text{if} \quad j = 1, k = 2, \quad \text{if} \quad j = 2, k = 1 \tag{5}$$

For the two-body TSS,

$$C > \left[l_{10}^e\Big/(1 + 1/f)\right]p_5 \tag{6}$$

where $p_5 = (1 + \beta_e')^2 + 2$.

TSS Spin Rate

We consider the TSS to be in an orbit of mean angular velocity Ω and all of the satellites to be in the orbital plane with the initial conditions of TSS spin rate β_0'. All satellites are aligned along the local vertical. By application of the tether deployment/retrieval, the tether length l_{j0}^s is changed to l_{j0}^f, $j = 1, 2$, and the TSS steady-spin rate changes to β_f'. Here, by the steady-spin motion we mean that the system spins with a constant average spin rate. Under the assumption that $l_{j0}^s \gg \hat{a}_{ij}, \hat{b}_{ij}, \hat{c}_{ij}$, the system initial and final angular momentums can be expressed approximately as

$$H_0 \approx mR^2\Omega + m\left[\mu_1(\mu_2 + \mu_3)l_{10}^{s2} + \mu_3(\mu_1 + \mu_2)l_{20}^{s2} + 2\mu_1\mu_3 l_{10}^s l_{20}^s\right]\Omega(1 + \beta_0') \tag{7}$$

$$H_f \approx mR^2\Omega + m\left[\mu_1(\mu_2 + \mu_3)l_{10}^{f2} + \mu_3(\mu_1 + \mu_2)l_{20}^{f2} + 2\mu_1\mu_3 l_{10}^f l_{20}^f\right]\Omega(1 + \beta_f') \tag{8}$$

where

$$\mu_1 = \frac{m_1}{m} = \frac{f_1}{1 + f_1 + f_1/f_2}, \quad \mu_2 = \frac{m_2}{m} = \frac{1}{1 + f_1 + f_1/f_2}$$

$$\mu_3 = \frac{m_3}{m} = \frac{f_1/f_2}{1 + f_1 + f_1/f_2}$$

m = total system mass $= m_1 + m_2 + m_3$.

Assuming the conservation of angular momentum $H_0 = H_f$ for the three-body TSS, we get

$$\beta_f' = \left[\frac{\mu_1(\mu_2 + \mu_3)l_{10}^{s2} + \mu_3(\mu_1 + \mu_2)l_{20}^{s2} + 2\mu_1\mu_3 l_{10}^s l_{20}^s}{\mu_1(\mu_2 + \mu_3)l_{10}^{f2} + \mu_3(\mu_1 + \mu_2)l_{20}^{f2} + 2\mu_1\mu_3 l_{10}^f l_{20}^f}\right] \times (1 + \beta_0') - 1 \tag{9}$$

and for the two-body TSS

$$\beta_f' = \left(l_{10}^s\Big/l_{10}^f\right)^2(1 + \beta_0') - 1 \tag{10}$$

As per Eqs. (9) and (10), during tether deployment the system spin rate decreases, and, thereby, the tether tension reduces and tethers may slacken. To find an initial spin rate to avoid tether slackening, we obtain the condition for the system rotational motion by simplifying the equation of motion for β_j [Eqs. (1)], assuming that $e = 0, \beta_j = \beta$, $j = 1, 2$ as

$$|\beta'| > \sqrt{3}|\cos\beta| \tag{11}$$

The solution of the equation of motion for $\beta_j = \beta$ in terms of elliptical functions considering $|\beta_0'| > \sqrt{3}$ is

$$\beta = \sin^{-1}\left\{sn\left[\beta_0'\theta, \left(\sqrt{3}\Big/|\beta_0'|\right)\right]\right\} \tag{12}$$

By the use of Eqs. (9–11), the condition of the system steady-spin motion for the tether deployment phase are obtained as follows: For a three-body TSS,

$$\beta_0' > \left(1 + \sqrt{3}|\cos\beta_f|\right) \times \left[\frac{\mu_1(\mu_2 + \mu_3)l_{10}^{s2} + \mu_3(\mu_1 + \mu_2)l_{20}^{s2} + 2\mu_1\mu_3 l_{10}^s l_{20}^s}{\mu_1(\mu_2 + \mu_3)l_{10}^{f2} + \mu_3(\mu_1 + \mu_2)l_{20}^{f2} + 2\mu_1\mu_3 l_{10}^f l_{20}^f}\right] - 1 \tag{13}$$

and for a two-body TSS,

$$\beta_0' > \left(1 + \sqrt{3}|\cos\beta_f|\right)\left(l_{10}^s\Big/l_{10}^f\right)^2 - 1 \tag{14}$$

For the tether retrieval, the condition of the system steady-spin motion is $\beta_0' > \sqrt{3}$. In the case of large tether deployment/retrieval, tether strains may affect the TSS spin rate, and, therefore, instead of Eq. (10), we consider the relation incorporating tether strains as

$$\beta_f' = \left(l_1^s\Big/l_1^f\right)^2(1 + \beta_0') - 1 \tag{15}$$

Using Eqs. (4) and (15), and carrying out suitable approximations, we get

$$\left[-\frac{(1 + 1/f_1)C}{l_{10,f}}\right]\left(l_1^f\right)^4 + \left[1 + \frac{\hat{b}_{21} - \hat{b}_{11}}{l_{10}^f}\right](1 + 1/f_1)C\left(l_{10}^f\right)^3 + \left(l_{10}^s\right)^4(1 + \beta_0')^2 = 0 \tag{16}$$

where

$$l_1^s = \frac{C(1 + 1/f_1)\left[l_{10}^s - \hat{b}_{11} + \hat{b}_{21}\right]}{C(1 + 1/f_1) - p_6 l_{10}^s}$$

$$p_6 = (1 + \beta_0')^2 - 1 + 3\cos^2\beta_0$$

Solving Eq. (16), we get l_1^f, and then, on substitution of l_1^f in Eq. (15), we obtain the final rotational rate β_f'. Next, we substitute β_f' into Eq. (4) to find the corresponding tether strain. Equations (10) and (15) are numerically integrated to obtain β_f.

Results and Discussion

To study the performance of the system, the detailed system response is numerically simulated by the use of Eqs. (1) with initial conditions of null satellite/tether attitude angles and corresponding nonzero attitude rates:

$$C = 10^8, \qquad K_1 = -0.5, \qquad K_2 = 0.3$$

$$\hat{r}_b = 2, \qquad f_1 = f_2 = 1, \qquad g_1 = g_2 = 1$$

$$\alpha_{i0} = \phi_{i0} = \gamma_{i0} = 0, \qquad i = 1, 2, 3$$

$$\beta_{j0} = \eta_{j0} = 0, \qquad l_{j0} = l_{jo,e}, \qquad j = 1, 2$$

$$\chi'_{i0} = 0.001, \qquad \phi'_{i0} = \gamma'_{i0} = 0.001, \qquad i = 1, 2, 3$$

$$\beta'_{j0} = \beta'_0 = \beta'_e, \qquad \eta'_0 = 0.001, \qquad l'_{j0} = l'_{je}, \qquad j = 1, 2$$

$$\hat{a}_{ij} = \hat{c}_{ij} = 0, \qquad \theta_{j0} = 0, \qquad \hat{Q}_q = 0$$

The integration is carried out using the International Mathematical and Statistical Library routine double-precision differentiable-algebraic system of equations Petzold–Gear (DDASPG) based on the Petzold–Gear back differentiation formulas (BDF) method.

We first study the effect of initial spin rate β'_0 on the system response of a two-body TSS moving in a circular orbit (Fig. 2 and Table 1). Because both of the satellites have similar mass and inertia properties, we show only the response of one of the satellites, for example, satellite 1. As β'_0 is increased from 2 to 20, the system response shows stable behavior, even for unfavorable mass distribution parameters in relation to a gravity-gradient configuration, with the attitude angles $|\chi_i|_{\max}$, $|\phi_i|_{\max}$, and $|\gamma_i|_{\max}$ decreasing from 0.12, 0.019, and 0.068 deg to 0.0016, 0.0027, and 0.0084 deg, respectively. The decrease in the amplitudes of satellite attitude angles is attributed to an increase in the tether strain from 1.12×10^{-5} to 4.52×10^{-4}. The period of oscillations of all of the attitude angles decreases drastically from 0.686 orbits to 0.005 orbits, which

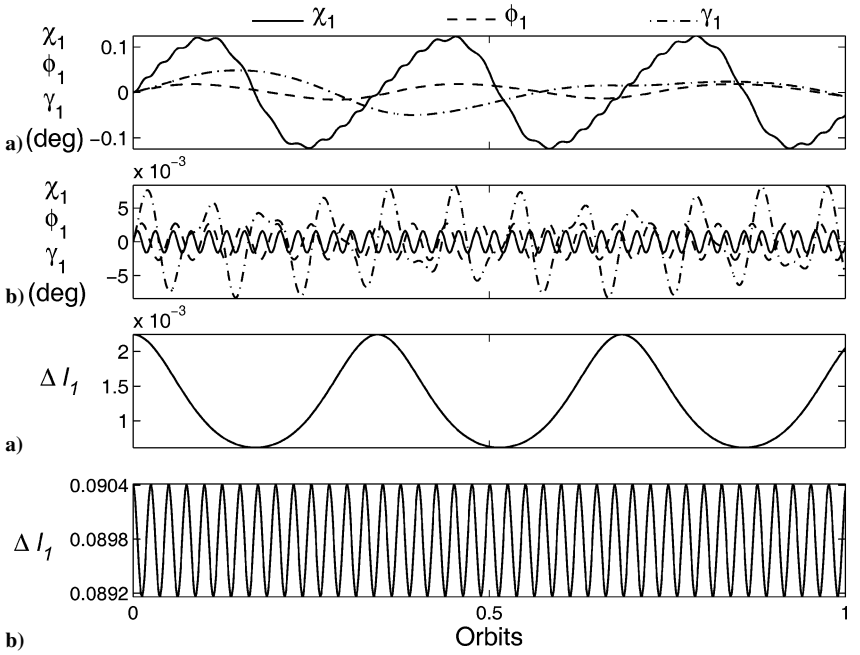

Fig. 2 Effect of in-plane swing rate β'_0 on two-body TSS with $\Delta I_1 = I_1 - 204$: a) $\beta'_0 = 2$ and b) $\beta'_0 = 20$.

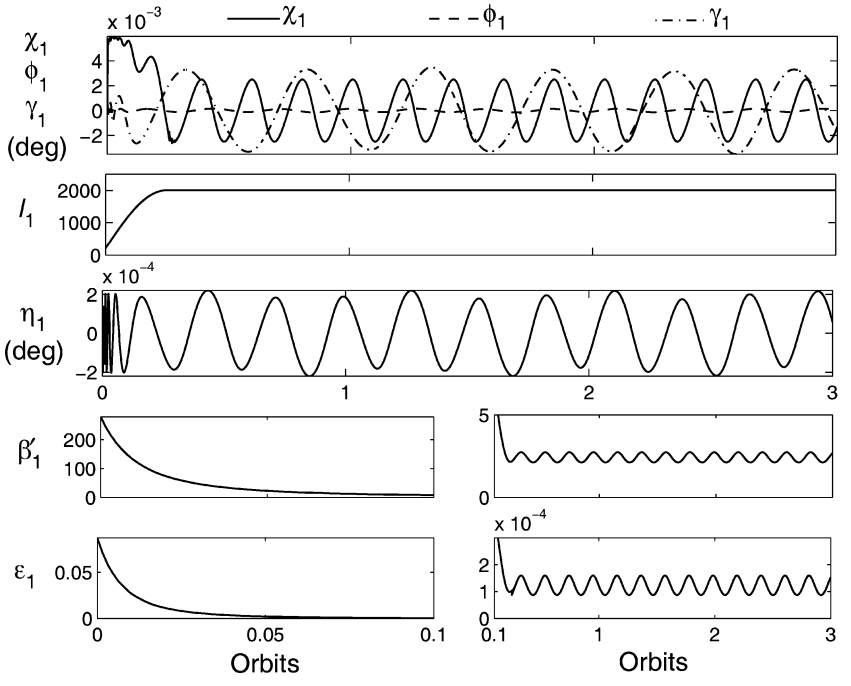

Fig. 3 System response of two-body TSS during tether deployment from 200 to 2000 in 0.25 orbit.

Table 1 Parameters for Figs. 2–5, for $I_{x1} = 500$ kg · m^2, $m_2 = 25$ kg, $\Omega = 0.0011$ rad/s, $L_{\text{ref}} = 4.5$ m, radial tether offset (r_b) = 9 m, and tether rigidity $EA = 1.4 \times 10^4$ N

Figure	e	β'_0	l^s_{j0} (L^s_{j0})	l^f_{j0} (L^f_{j0})	Controller gains
2	0	2 or 20	200 (900 m)	200 (900 m)	$\mu_\alpha = \nu_\alpha = \mu_\phi = \nu_\phi = \mu_l = \nu_l = 0$
3	0	280	200 (900 m)	2000 (9000 m)	$\mu_\alpha = 0.0025$, $\nu_\alpha = 2.9$, $\mu_\phi = 0.001$, $\nu_\phi = 1$, $\mu_l = 10$, $\nu_l = 0.002$
4	0	2	1000 (4500 m)	500 (2250 m)	$\mu_\alpha = 0.1$, $\nu_\alpha = 1$, $\mu_\phi = 0.05$, $\nu_\phi = 5$, $\mu_l = \nu_l = 0$
5	0.05	2	1000 (4500 m)	500 (2250 m)	$\mu_\alpha = 0.2$, $\nu_\alpha = 1$, $\mu_\phi = 0.05$, $\nu_\phi = 5$, $\mu_l = \nu_l = 0$

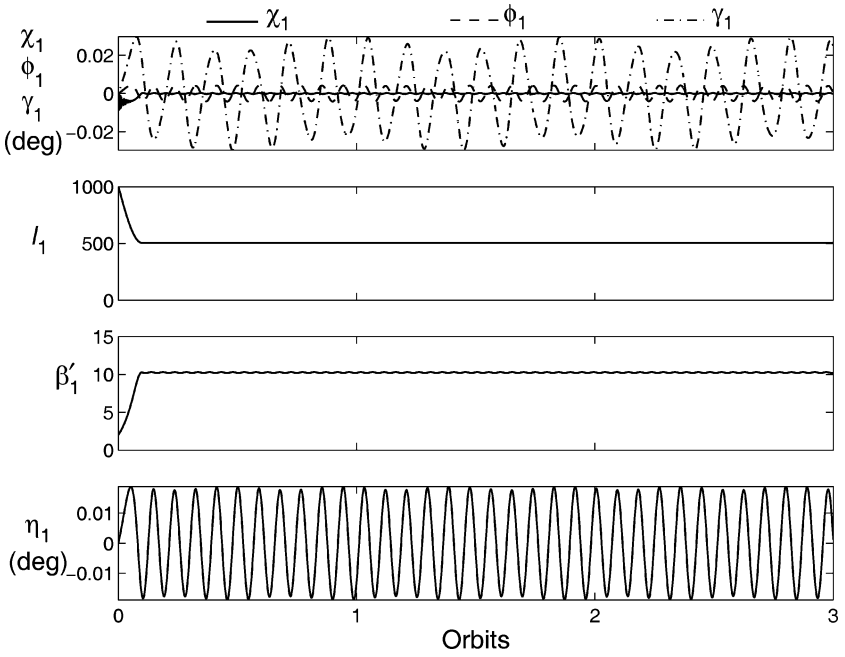

Fig. 4 System response of three-body TSS during tether retrieval from 1000 to 500 in 0.1 orbit.

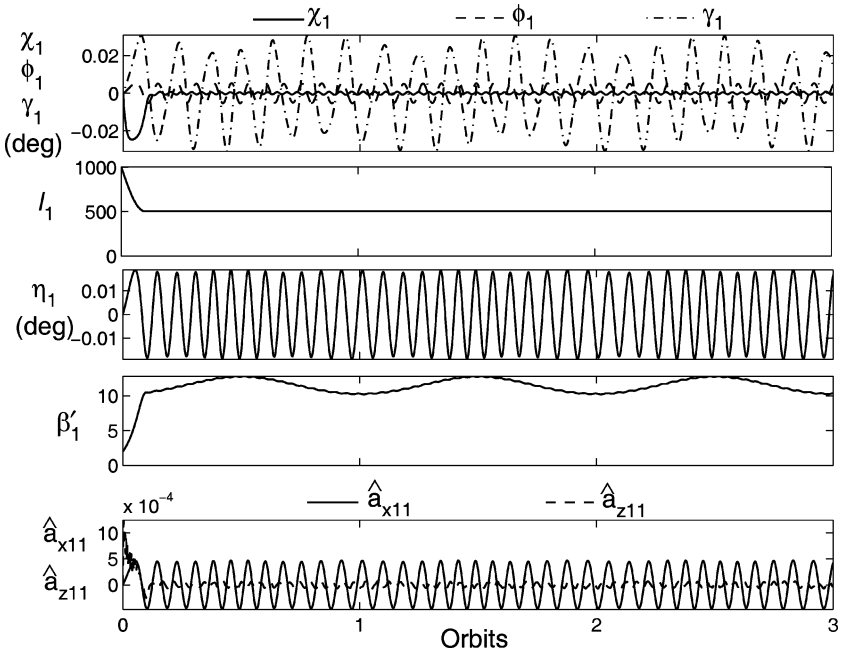

Fig. 5 System response of two-body TSS in presence of eccentricity during tether retrieval from 1000 to 500 in 0.1 orbit.

matches analytically with a β_1 response as per Eq. (12). The period of tether oscillations, with reference to Eq. (4), is one-half of the period of β_1. The decrease in the period of tether oscillations leads to a decrease in the period of the satellite attitude oscillations. The tether length/offset affects the system response significantly. As β_0' is increased from 2 to 20, the critical tether length and offset decrease from 60 (for $\hat{r}_b = 2$) and 0.4 (for $l_{t0} = 200$) to 0.8 and 0.004, respectively.

Next, we study the effect of tether deployment on a two-body TSS. The system amplitudes become quite high during deployment, and, therefore, we apply a tether offset control, scheme along with tension control, as follows:

$$\hat{a}_{ij} = (-1)^i[\mu_\alpha \alpha_i' + \nu_\alpha \alpha_i], \qquad \hat{c}_{ij} = (-1)^{i+1}[\mu_\phi \phi_i' + \nu_\phi \phi_i]$$

$$\hat{b}_{ij} = (-1)^i\left[\hat{r}_{ij}^2 - \hat{a}_{ij}^2 - \hat{c}_{ij}^2\right]^{\frac{1}{2}}, \qquad j = 1, 2, 3, \qquad i = j, j+1$$

$$\hat{Q}_{l_j} = -\mu_l(l_j' - l_{j0}') - \nu_l(l_j - l_{j0} - 2|\hat{b}_j|), \qquad j = 1, 2 \quad (17)$$

where μ_t and ν_t, $t = \alpha, \phi, l$, are derivative and proportional gains.

By application of the control strategy [Eq. (17)], the system response becomes stable with steady-state attitude angles of $|\chi_i|_{\max} = 2.5 \times 10^{-3}$ deg, $|\phi_i|_{\max} = 1.5 \times 10^{-4}$ deg, $|\gamma_i|_{\max} = 3.5 \times 10^{-3}$ deg, $i = 1, 2$, and $|\eta_1|_{\max} = 2.2 \times 10^{-4}$ deg (Fig. 3). The period of tether oscillations at the end of deployment is 0.207 orbits. That corresponds to $\beta_f' = 2.735$ using Eq. (12), and the simulation verifies exactly the same value of β_f'. The tether oscillations cannot become further reduced because they represent steady-spin motion, and they induce relative satellite pitch oscillations of the same period. During the tether deployment, β' decreases from an initial value of 280 to 2.12 [analytical value 1.65 using Eq. (10) and 2.25 using Eq. (15)] at the end of deployment. Correspondingly, the initial tether strain 0.0875 also decreases to 8.7×10^{-4} [analytical value 6.02×10^{-5} using Eq. (10) and 9.58×10^{-4} using Eq. (15)]. The upper and lower limits derived on β_0' are 272 and 99 [Eq. (10)] and 238 and 100 [Eq. (15)]. By the use of the proposed control scheme, the system is stable only for such initial β_0' where $\beta_f' > \sqrt{3}|\cos\beta_f|$. In the case of tether retrieval of a three-body TSS (Fig. 4), the system remains stable with β_j' and tether strain ε_j increases progressively from an initial value of 2 and 1.5×10^{-4} to 10.3 [analytical value, 11 using Eq. (15)] and 7.8×10^{-4} [analytical value 1×10^{-3} using Eq. (3)], respectively, at the end of retrieval. All three satellites have virtually similar responses because they are of similar mass and inertia properties, and, therefore, only response plots for satellite 1 are shown in Fig. 4. Even in the presence of eccentricity as high as 0.05 (Fig. 5), the proposed control scheme results in high system performance. For the case of the out-of-plane swing rate η_0', if η_0' is relatively low compared to β_0', the system response remains unaffected with the η_j response bounded.

Conclusions

The dynamics and control of a rotating linear array TSS are presented. In a stationkeeping phase, a critical spin rate for the multibody TSS with flexible tethers remains the same as that of a two-body TSS with a rigid tether. The tether length/offset has a significant effect on the TSS response. However, the system remains stable even with a relatively smaller tether length/offset as compared to the tether length/offset needed for the stable motion of a nonspinning TSS. During tether deployment/retrieval, the TSS spin rate changes, and the tether flexibility has a significant effect on it. The TSS spin rate derived analytically considering tether flexibility matches more closely with the numerical simulation as compared to the case of a rigid tether. The tether rigidity C has an effect on the TSS response, and its critical value is derived. The tether offset control laws augmented with tether tension control are successful in controlling satellite attitude, as well as tether oscillation during tether deployment/retrieval if $\beta' > \sqrt{3}|\cos\beta|$. Finally, the results of the numerical simulation establish the feasibility of achieving a rotating linear array formation for multiple satellites of any desired aperture size.

References

[1]DeCou, A. B., "Attitude and Tether Vibration Control in Spinning Tethered Triangles for Orbiting Interferometry," *Journal of the Astronautical Sciences*, Vol. 41, No. 3, 1993, pp. 373–398.

[2]Tragesser, S. G., "Formation Flying with Tethered Spacecraft," AIAA Paper 2000-4133, Aug. 2000.

[3]Williams, T., and Moore, K., "Dynamics of Tethered Satellite Formations," *Advances in the Astronautical Sciences*, Vol. 112, Pt. 2, 2002, pp. 1219–1235.

[4]Quadrelli, M. B., "Modeling and Dynamics Analysis of Tethered Formations for Space Interferometry," *Advances in the Astronautical Sciences*, Vol. 108, Pt. 2, 2001, pp. 1259–1278.

[5]Bombardelli, C., Lorenzini, E. C., and Quadrelli, M. B., "Pointing Dynamics of Tethered-Controlled Flying for Space Interferometry," *Advances in the Astronautical Sciences*, Vol. 109, Pt. 2, 2001, pp. 1539–1552.

[6]Kumar, K. D., "Line-of-Sight Pointing of Multiple Micro-Satellites in Non-Equatorial Orbits," International Astronautical Congress, Paper IAC-02-M.4.06, Oct. 2002.

D. Spencer
Associate Editor